MINERALOGICAL MAGAZINE, DECEMBER 1980, VOL. 43, PP. 995-1003

Hibonite and coexisting zoisite and clinozoisite in a calc-silicate granulite from southern Tanzania

P. MAASKANT, J. J. M. M. M. COOLEN, AND E. A. J. BURKE

Institute of Earth Sciences, Free University, De Boelelaan 1085, 1081 HV Amsterdam, The Netherlands

SUMMARY. The third terrestrial occurrence of hibonite is reported from granulite-facies rocks in the Furua Granulite Complex in southern Tanzania. The mineral forms yellowish-brown lath-shaped crystals in a grossular-anorthite rock containing subordinate sphene (clino)zoisite, hercynite, apatite, ilmenite, and corundum-ilmenite intergrowths.

Electron-microprobe analyses indicate a generalized formula $(Ca_{1-x}RE_x)[(Al,Fe^{3+})_{12-2a+x}(Ti,Si)_{a-x}(Fe^{2+},Mg)_a]O_{19}$, with $RE = Ce+La+Nd$, $x = 0.2$, and $a = 0.8$. Individual mineral analyses show a cation substitution of $Ca+Ti+Fe^{3+} = RE+2Al$. Relatively high *RE* and Fe contents represent the main chemical differences with meteoritic hibonite. The hexagonal unit cell has $a = 5.61$ Å, $c = 22.18$, in good agreement with the other terrestrial hibonites.

Three compositional types of (clino)zoisite are distinguished: 1.8-3.1 wt% Fe_2O_3 (orthorhombic and monoclinic), 3.9-6.0 wt% Fe_2O_3 (monoclinic), and 5.8-7.9 wt% Fe_2O_3 with an average of 6.3 wt% RE_2O_3 (monoclinic).

Thermometric and barometric data for coexisting pyroxenes and garnet from adjacent rocks indicate granulite-facies equilibration conditions of 750 to 850 °C and 6 to 11 kb. During retrogression with increasing partial H_2O pressures, hibonite reacted with plagioclase and garnet to form spinel, sphene, and *RE*-bearing clinozoisite. Corundum-ilmenite intergrowths probably resulted from the breakdown of an Fe-högbomite.

THE rare mineral hibonite, with the theoretical composition of $CaO{\cdot}6Al_2O_3$, is well known from Ca-Al-rich inclusions in carbonaceous chondritic meteorites (Keil and Fuchs, 1971; Blander and Fuchs, 1975; Macdougall, 1979; Smith, 1979). In the Allende and Leoville meteorites, for instance, hibonite occurs in association with anorthite, perovskite, gehlenite, spinel, wollastonite, andradite, and fassaite. Textural, thermodynamic, and isotopic anomaly data suggest that hibonite in meteorites may be regarded, at least in several cases, as an early high-temperature condensate from a primitive solar nebula (Shimizu *et al.*, 1978; Smith, 1979; Lorin, pers. comm.).

The presence of hibonite in terrestrial rocks, however, has been reported only twice. Curien *et al.* (1956) described the mineral from an alluvial deposit and a metamorphic limestone in Madagascar; the limestone is rich in calcic plagioclase and contains minor amounts of corundum, spinel, and thorianite. Hibonite also occurs in Gornaya Shoriya, Siberia, in siliceous marbles of the Proterozoic Konzhin suite (Kuzmin, 1960; Yakovlevskaya, 1961). This suite consists of amphibolites, garnet-biotite gneisses, and marbles with a varying dolomite content. Mineral parageneses are indicative of the amphibolite facies of metamorphism. Calc-silicates have been formed in the marbles by metasomatic processes which are related to the migmatization of the amphibolites and gneisses (Letuvninkas, 1971). Dolomite-rich marbles give assemblages with chondrodite, spinel, and phlogopite. Calcite-rich marbles give fine- to medium-grained rocks with disseminated streaks and nests of non-carbonate minerals, mainly idocrase, with minor amounts of hibonite, hercynite, corundum, andalusite, kyanite, diopside, rutile, sphene, and magnetite. Hibonite forms tabular and platy crystals with an average size of 5 to 10 mm, rarely up to 20 mm. The hibonite content in individual streaks and nests may reach 35 to 50 vol.%.

The present study deals with a new occurrence of the mineral in the Furua Granulite Complex in southern Tanzania. This complex forms a part of the five Quarter Degree Sheets (264, 265, 275, 276, 277) which were mapped in the early 1970s by two Amsterdam petrology departments in co-operation with the Mineral Resources Division of the Ministry of Commerce and Industry of Tanzania. The complex is situated south-west of Mahenge in the northern parts of QDS 264 and 265, and in the adjacent areas of QDS 250 and 251. Hibonite was discovered in a calc-silicate rock in the course of a detailed geochemical and petrological investigation of the granulites (Coolen, 1980).

Geological setting. The Furua Granulite Complex is a part of the Upper Proterozoic Mozambique mobile belt, which extends along the eastern

side of the African continent. A detailed description of this belt is given, among others, by Kröner (1977, 1979). The southern part of the Mozambique belt mainly consists of intermediate- to high-grade metamorphic rocks. The presence of large domains of granulite-facies metamorphics is characteristic. In Tanzania these granulites form a discontinuous, roughly north-south trending zone in the central part of the Mozambique belt. Hepworth (1972) refers to these rocks as the 'Eastern Granulites'. The granulites and the surrounding amphibolite-facies rocks belong to the Usagaran System, a succession of predominantly metasedimentary rocks (Quennel *et al.*, 1956). Structural and radiometric age relationships between the granulites and the surrounding rocks are not yet fully understood (Hepworth, 1972). The age of the Usagaran gneisses from central and south-western Tanzania is in the range of 1750 to 1900 Ma (Wendt *et al.*, 1972; Priem *et al.*, 1979). In eastern direction the gneisses were progressively rejuvenated by the influence of the Pan-African thermotectonic episode, resulting in ages around 500 to 600 Ma.

A banded Usagaran gneiss from a locality 10 km south-west of the boundary with the Furua Granulite Complex gives an internal Rb/Sr isochron age of 589 ± 70 Ma (Priem *et al.*, 1979). No radiometric data are as yet available for the Furua granulites. Rb/Sr ages of comparable 'Eastern Granulites' from the northern part of Tanzania are in the range of 730 to 930 Ma (Spooner *et al.*, 1970). The Furua Granulite Complex consists of high-grade polymetamorphic rocks with a wide compositional range. Banded hornblende-pyroxene granulites, generally garnet- and scapolite-bearing, predominate (Coolen, 1980). The mineral parageneses are indicative of the hornblende-orthopyroxene-plagioclase and the hornblende-clinopyroxene-almandine granulite subfacies. On the basis of two-pyroxene-garnet compositional data temperatures of 750 to 850 °C and load pressures of 6 to 11 kb are inferred for the physical conditions during the main phase of granulite-facies metamorphism. Retrograde metamorphism of the granulites is a common feature, though generally restricted to well-defined zones. The boundary between the Furua Granulite Complex and the adjacent region of acid gneisses is formed mainly by a major fault.

Occurrence. Hibonite occurs in a calc-silicate rock from a unit of granulites and gneisses in the central part of the complex. This unit forms a 1.5-km-wide zone along the western offshoots of Ligamba hill and consists of a banded series of graphite-bearing leuco- to mesocratic biotite-garnet gneisses, clinopyroxene-garnet granulites, quartzites, and subordinate amounts of two-pyroxene granulites. The hibonite-bearing calc-silicate rock occurs in the central part of this presumably sedimentary series. The location coordinates of the sample (collection number C-76) are 9° 02′ 40″ S and 36° 24′ 40″ E. Loose blocks of calc-silicate rock, up to several decimeters in size, occur in a small, at least 10 m wide, zone of a badly exposed river section. The rock is medium-grained, non-foliated, and brown-grey in colour.

Petrography and mineralogy. Anorthite ($An_{99.4}Ab_{0.5}Or_{0.1}$) and grossular ($Gr_{74.6}Andr_{2.6}Alm_{21.8}Spess_{0.4}Pyr_{0.6}$, with 1.0 wt% TiO_2) form about 90 vol.% of the hibonite-bearing calc-silicate rock. The unzoned, polysynthetically twinned plagioclase and the homogeneous garnet are medium-grained, forming a granoblastic texture. Sphene, zoisite, and clinozoisite are the principal minor constituents. Sphene (with about 3 wt% Al_2O_3 in a semiquantitative analysis) is present as fine-grained anhedral subangular grains. Three compositional types of (clino) zoisites, low-Fe, intermediate-Fe, and high-Fe types, have been distinguished on the basis of microprobe analyses (Table I).

The low-Fe type is represented by medium-grained anhedral, sometimes poikilitic zoisite, and by subhedral prismatic zoisite and clinozoisite. The poikilitic zoisite seems to have formed at the expense of plagioclase and/or garnet. Zoisite shows anomalous bluish and brownish interference colours, a strong dispersion $r \ll v$, $2V_\gamma$ (measured) of about 30° in red light and 40° in blue light, OAP // (100) with deviations up to 20° (confirming the findings of Ackermand and Raase, 1973), and usually a positive elongation in prismatic sections. X-ray diffraction patterns of eleven individual grains of low-Fe type (clino)zoisites have been determined. The patterns of five poikilitic grains and four prismatic grains reveal an orthorhombic symmetry whereas the patterns of two prismatic grains reveal a monoclinic symmetry.

The intermediate-Fe type clinozoisite, present as reaction rims between garnet and plagioclase and as fine-grained subhedral prisms, always shows bluish interference colours, parallel extinction, and a negative elongation. A monoclinic symmetry is attributed to this type because it is believed that Fe-contents of that order cannot be incorporated in an orthorhombic unit cell.

The high-Fe-type clinozoisite, containing also appreciable amounts of *RE*, generally occurs as interstitial and relict grains which suggest that this type of clinozoisite is relatively older. The mineral is nearly always surrounded and replaced by a rim of intermediate-Fe clinozoisite. This high-Fe allanitic clinozoisite is commonly polysynthetically

twinned || (100), showing symmetrical extinction and alternating positive and negative elongation in appropriate sections; twinning often extends within the surrounding intermediate-Fe clinozoisite rim. *RE*-contents may vary within a single grain, causing patchy interference colours.

Green hercynite spinel $(Mg_{0.04}Fe^{2+}_{0.96})(Al_{1.88}Fe^{3+}_{0.11}Ti_{0.004})O_4$, occurs as anhedral lobate grains and as inclusions in garnet. Corundum is present as a few lath-shaped grains, crowded with ilmenite grainlets and surrounded by intermediate-Fe clinozoisite (fig. 1). It is also present as small inclusions in garnet. The intergrowths of corundum and ilmenite were probably formed by way of a breakdown of a formerly homogeneous Fe-Ti-Al-oxide phase, which most likely was Fe-högbomite. Compositions of högbomite with Fe/(Fe + Mg) higher than 0.7 are unknown in nature. Moore (1971) suggested that Fe-högbomite is stable only at elevated *PT*-conditions, and that dissociation to corundum and ilmenite will take place at lower temperatures and pressures. An origin of the intergrowths by alteration of hibonite is considered unlikely because the hibonite crystals in the sample show no evidence of such a process. The volumetric ratio ilmenite/corundum in the intergrowths is about 0.25, which is in agreement with the calculated compositional parameters of Fe-högbomite.

Hibonite occurs as laths and stringers, with an average length and width of 0.5 and 0.05 mm respectively, often included in a subparallel alignment in garnet (fig. 2). The mineral is apparently unstable in a (clino)zoisite environment, in which it reacts to form spinel, *RE*-bearing clinozoisite, and sphene. X-ray emission distribution pictures (fig. 3*a–d*) demonstrate this relationship. The hibonite grains occasionally show rims of green spinel. In thin section hibonite has a yellowish-brown colour, which decreases in intensity with rising *RE* contents, as revealed in a zoned basal

TABLE I. *Electron-microprobe analyses of zoisite and clinozoisite*

	Low-Fe zoisite and clinozoisite		Intermediate-Fe clinozoisite		High-Fe, *RE*-clinozoisite	
Wt.%	n = 11	range	n = 10	range	n = 8	range
SiO_2	38.6	38.4–39.2	38.5	38.0–38.9	36.6	36.3–36.8
Al_2O_3	31.9	31.6–32.2	29.9	28.8–30.2	27.7	27.0–28.3
TiO_2	0.23	—	0.20	—	0.24	—
Fe_2O_3*	2.2	1.8– 3.1	4.6	3.9– 6.0	2.6	5.8 –7.9
FeO	—		—		3.0	—
CaO	24.1	23.7–24.2	23.8	23.5–24.2	20.5	19.2–21.6
Ce_2O_3	—		—		3.0	2.4– 4.0
La_2O_3	—		—		1.8	1.0– 2.8
Nd_2O_3	—		—		1.5	—
Total	97.03		97.00		96.94	
Cations on 25 oxygen atoms						
Si	5.96		5.99		5.97	
Al	5.77		5.49		5.32	
Ti	0.027		0.023		0.028	
Fe^{3+}	0.26		0.53		0.30	
Fe^{2+}	—		—		0.42	
Ca	3.99		3.97		3.58	
Ce	—		—		0.18	
La	—		—		0.11	
Nd	—		—		0.09	
Total	16.00		16.00		16.00	
Pistacite content	4.3		8.8			

n = number of determinations.

* In low-Fe and intermediate-Fe varieties all Fe is assumed to be present in the trivalent state; in *RE*-bearing types Fe^{3+}/Fe^{2+} ratios are calculated on a basis of sixteen cations.

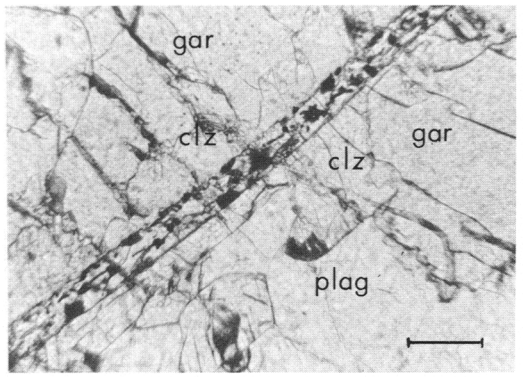

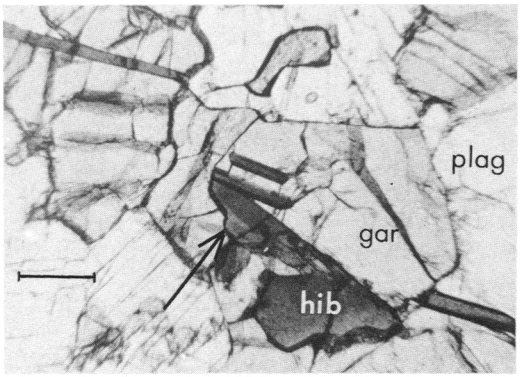

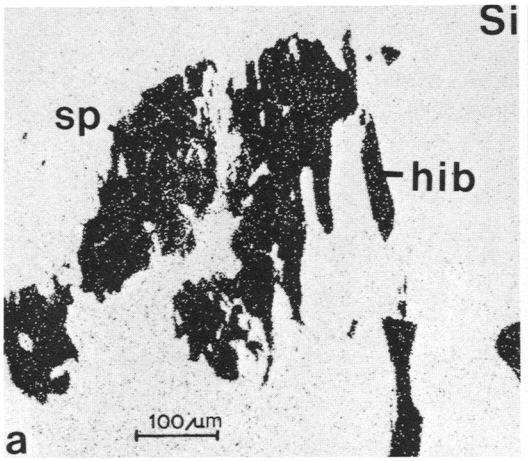

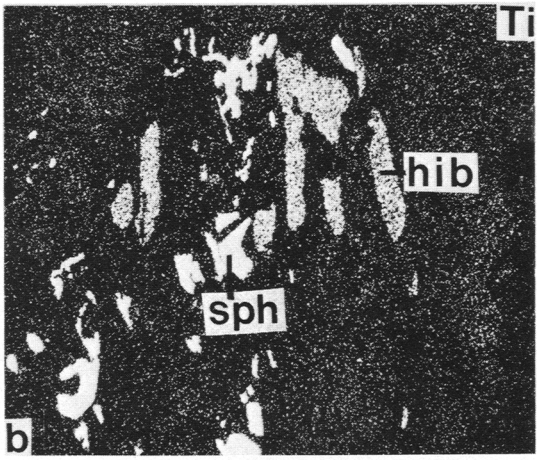

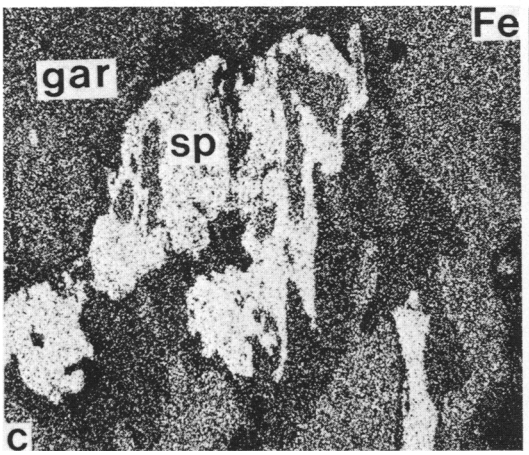

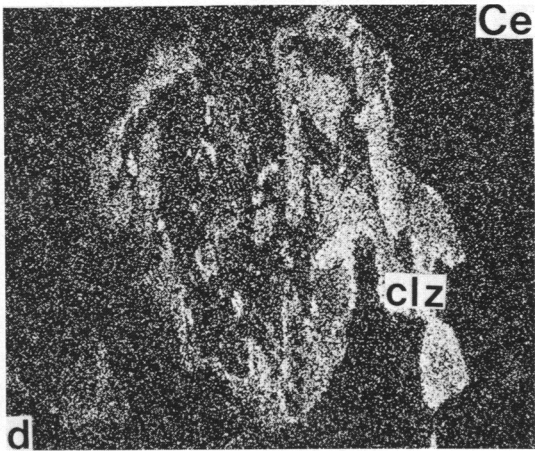

FIGS. 1–3. FIG. 1 (*top left*). Lath-shaped corundum with enclosed ilmenite, rimmed by clinozoisite (clz) in a garnet (gar)–plagioclase (plag) surrounding. Length of bar 60 µm. FIG. 2 (*top right*). Hibonite (hib) within garnet. Arrow indicates the position and direction of the scanning profile of fig. 4. Bright and dark areas correspond to *RE*-rich and *RE*-poor areas, respectively. Length of bar 250 µm. FIG. 3 (*below*). X-ray emission images (3a–d) for Si, Ti, Fe, and Ce radiation respectively, showing replacement of hibonite (hib) by spinel (sp), sphene (sph), clinozoisite (clz) within garnet (gar). Hibonite remnants are best seen on the Ti image. Note the irregular distribution of Ce in the newly formed high-Fe type clinozoisite.

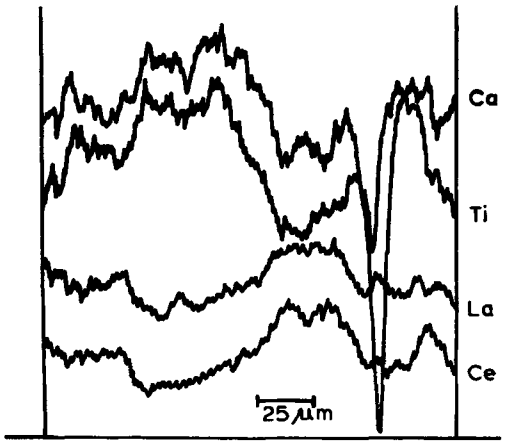

FIG. 4. Scanning profile across the basal section of hibonite shown in fig. 2.

section (figs. 2 and 4). Pleochroism, as shown by the hibonites from Madagascar and Siberia, has not been observed. Curien *et al.* (1956) note a pleochroism from brownish grey (ω) to grey (ε) whereas Letuvninkas (1971) notes a pleochroism from brownish yellow (ω) to yellow (ε). The hexagonal mineral is uniaxially negative, and shows a positive elongation and a perfect basal cleavage in prismatic sections. Cathodoluminescence in red and blue colours, described from the Allende and Leoville hibonite, has not been noticed under 30 kV and 100 nA electron-beam conditions.

Mineral chemistry. Electron-microprobe analyses were performed with Cambridge Instruments Geoscan (with a LINK energy-dispersive system) and Microscan 9. All microprobe data presented in this paper were obtained with the wavelength-dispersive method. Natural compounds and synthetic *RE*-bearing glasses were used as standards. The analytical conditions were chosen so as to obtain counting statistics with 2σ values of about 1% for the major elements. Apparent concentrations were ZAF-corrected with the Springer (1967) program modified by Kieft and Maaskant (1969), and with the Microscan 9 on-line ZAF program.

The average data for plagioclase, garnet, and spinel are mentioned already in the description of the minerals. Table I shows the analyses of zoisite and clinozoisite. The existence of a compositional gap between the low-Fe type and the intermediate-Fe type is evident. The position and width of this gap are in agreement with the data of Ackermand and Raase (1973), who did not measure compositions between 2.6 and 4.2 wt% Fe_2O_3. This compositional gap apparently does not correspond with a distinct change in crystal structure because optical deviations from the orthorhombic symmetry were observed, and two grains of the low-Fe type gave X-ray powder diffraction patterns with monoclinic symmetry. Optical and chemical data for the orthorhombic low-Fe type match those given by Myer (1966) for ferrian zoisite, and by Tröger (1971) for α-zoisite. Based on the assumption of stoichiometry all iron in both *RE*-free (clino)zoisites is present in the trivalent state. The *RE* content of the high-Fe type clinozoisite is rather high, although much lower than in allanite. Its chemical composition does not compare well with the rather restricted compositional range of allanite (Hasegawa, 1960). Hence, this type is named allanitic clinozoisite to account for the *RE* content in combination with the presence of substantial amounts of divalent iron and for the low $Fe^{3+}/(Fe^{3+}+Al)$ ratio with respect to the clinozoisite–epidote series.

Fourteen grains of hibonite were analysed; average weight percentages, compositional range, and average cation numbers (on the basis of a cation total = 13, and O = 19) are presented in Table II. The cation numbers of the individual analyses are graphically displayed in fig. 5. The various curves illustrate well-defined sympathetic and antipathetic trends, and the curve of the calculated ferric ion values, moreover, resembles the total-Fe curve in a way indicating the following cation substitution: $Ca+Ti+Fe^{3+} \rightleftharpoons RE+2Al$, see also fig. 4. This

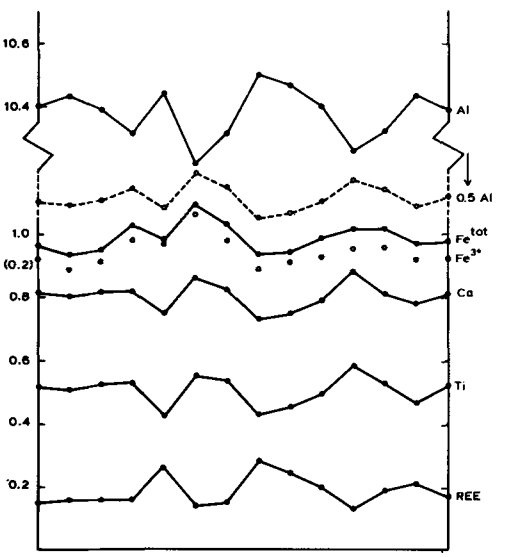

FIG. 5. Cation numbers of 14 hibonite grains, calculated on a basis of O = 19 and sum cations = 13. A reverse 0.5 Al curve shows similar trends to the other curves. Note the position of the calculated Fe^{3+} cation numbers in relation to the Fe^{tot} curve.

TABLE II. *Chemical analyses of hibonite from Tanzania (this study), Madagascar* (a) *this study;* (b) *(Curien* et al., *1956), and Siberia (Yakovlevskaya, 1961)*

	Tanzania		Madagascar		Siberia
Wt.%	n = 14	range	a	b	
SiO_2	0.75	0.67- 0.80	0.6	1.50	1.03
Al_2O_3	72.8	72.1 -73.6	76.1	74.00	73.67
TiO_2	5.6	4.7 - 6.4	6.3	8.50	5.10
Fe_2O_3	2.7*	1.9 - 4.0	1.9*	0.45	9.90
FeO	7.3†	7.0 - 7.6	2.5	2.30	0.35
MgO	0.27	0.20- 0.31	2.8	3.20	1.59
CaO	6.2	5.6 - 6.8	7.5	6.50	8.67
Ce_2O_3	2.1	0.8 - 3.2	0.2	}	n.d.
La_2O_3	1.8	1.5 - 2.1	—	} 3.50‡	n.d.
Nd_2O_3	0.2	—	0.1	}	n.d.
ThO_2	—		1.5	§	n.d.
Total	99.72		99.5	99.95	100.31
Cations on 19 oxygen atoms					
Si	0.09		0.07	0.19	0.12
Al	10.38		10.49	10.18	10.12
Ti	0.51		0.55	0.74	0.45
Fe^{3+}	0.25		0.17	0.04	0.87
Fe^{2+}	0.74		0.24	0.23	0.03
Mg	0.05		0.49	0.56	0.28
Ca	0.80		0.94	0.81	1.08
Ce	0.09		0.008	}	—
La	0.08		—	} 0.16	—
Nd	0.01		0.004	}	—
Th	—		0.04	—	—
Total	13.00		13.00	12.91	12.95

n = number of determinations.
n.d. = not determined.
— = *not found.*
* Fe_2O_3 contents are calculated on a basis O = 19 and sum of cations = 13.
† Range in total Fe, calculated as FeO, is 9.2–10.8 wt% with an average value of 9.7 wt%.
‡ Curien *et al.* (1956) give *RE*-oxide totals.
§ Curien *et al.* (1956) state: 'La radioactivité du minéral est très faible, 1000 ppm en Th et 100 ppm en U.'

site- and valency-balanced equation is the sum of two common substitutions: (1) $Ca + Fe^{3+} \rightleftharpoons RE + Fe^{2+}$, and (2) $Ti + Fe^{2+} \rightleftharpoons 2Al$. The former substitution is well known from the allanite-epidote series, and the latter is found in meteoritic hibonites (with Mg in the place of Fe^{2+}; Lorin and Christophe Michel-Lévy, unpublished data), and is also common in rock-forming silicates. Deviations from unity for Ca, *RE*, or Ti in the simple substitutions will lead to the presence of Fe^{2+} at the left or right side of the substitution equation for hibonite. The average composition of the Tanzania hibonite is

$$(Ca_{0.80}RE_{0.18})[Al_{10.38}Fe^{3+}_{0.25}(Ti,Si)_{0.60}(Fe^{2+},Mg)_{0.79}]O_{19}. \quad (1)$$

Taking into account the above-mentioned cation substitution this leads to a generalized formula

$$(Ca_{1-x}RE_x)[(Al,Fe^{3+})_{12-2a+x}(Ti,Si)_{a-x}(Fe^{2+},Mg)_a]O_{19}, \quad (2)$$

with $a = 0.8$ and $x = 0.2$.

It should be stressed, however, that this formula is not necessarily valid for the other hibonites. This is mainly caused by the impossibility of distinguishing between ferrous and ferric iron in electron-microprobe analysis. In this case ferric iron contents have been calculated on the basis of O = 19 and a sum of cations = 13, because the structure of hibonite is similar to those of magnetoplumbite ($PbO \cdot 6Fe_2O_3$) and synthetic $CaO \cdot 6Al_2O_3$ (Curien *et al.*, 1956). It remains a question whether the cation substitution is site-balanced. It is indeed possible that the common substitution $2(Mg, Fe^{2+}) \rightleftharpoons Ti$ is also operative in this system. This would imply that the ferric iron content of hibonite cannot be calculated at all, because the sum of cations will deviate unpredictably and arbitrarily from 13 in a formula

$$[(Ca_{1-x}RE_x)(Al,Fe^{3+})_{12-2a+x}(Ti,Si)_{a-x\mp z}(Fe^{2+},Mg)_{a\pm 2z}]_{13\pm z}O_{19}. \quad (3)$$

The analysis of the Madagascar hibonite, as given by Curien *et al.* (1956), indicates the possibility of such a substitution with (Ti,Si) = 0.93 and (Fe^{2+}, Mg) = 0.79. An electron microprobe analysis of a large hibonite crystal from Esiva, Madagascar, shows relatively high Th and low *RE* contents. Taking into account the valency difference between Th and *RE* the generalized hibonite formula (2) may be applied to this analysis.

Further complications will arise if the reliability of the analyses is questioned, the ratio $CaO : 6Al_2O_3$ varies within certain limits, or if a multi-site exchange between (Fe^{2+},Mg) and Ca, and between *RE* (or other large-sized ions such as Th) and (Al,Fe^{3+}) is considered possible. These factors probably apply to compositional data (based on O = 19) of the Siberia and some meteoritic hibonites. The analyses of hibonite from Gornaya Shoriya, formerly described as högbomite (Kuzmin, 1960), will not be taken into consideration because of the first-mentioned factor. An analysis of the same hibonite given by Yakovlevskaya (1961), see Table II, shows an excess of Ca which will be further enhanced if contents of *RE* and/or other large-sized ions are added to the Ca site. These elements were not analysed, but should be present in view of the reported similar unit-cell dimensions (Table IV). An excess of Ca is also frequently reported for meteoritic hibonite (Keil and Fuchs, 1971; Macdougall, 1979).

X-ray data. X-ray powder diffraction data were obtained using a Straumanis-type 114.57 mm Debye-Scherrer camera (Mn-filtered Fe-K_α radiation). The mineral was powdered under the microscope with a tungsten carbide microdrill and taken into droplets of rubber solution, which considerably darkens the film in the region for d greater than 3 Å. Some lines of WC were present on the films because the hardness of hibonite is about $8\frac{1}{2}$. The pattern (Table III) is identical to the hibonite patterns published by Keil and Fuchs (1971). The hexagonal unit-cell constants (obtained from a least-squares analysis of twelve reflections) are comparable to those of the other terrestrial occurrences, but differ from meteoritic hibonite (Table IV). The higher c-values in terrestrial hibonites can be explained by substitution of Ca by larger-sized ions, such as *RE* or Th, in these hibonites.

TABLE III. *X-ray powder diffraction data for hibonite from Tanzania*

hkil	d_{calc} Å	d_{obs} Å	*I*	*hkil*	d_{calc} Å	d_{obs} Å	*I*
0004	5.54	—	—	$20\bar{2}9$	1.730	—	—
$01\bar{1}2$	4.45	4.44	1	$02\bar{2}10$	1.638	1.637	2
$01\bar{1}3$	4.06	—	—	$03\bar{3}0$	1.620	1.622	1
0006	3.70	—	—	$21\bar{3}7$	1.589	1.590	3
$01\bar{1}6$	2.942	2.954	3	00014	1.584	1.579	2
$11\bar{2}0$	2.805	2.812	6	$03\bar{3}3$	1.582		
$11\bar{2}2$	2.720	—	—	$03\bar{3}4$	1.555	1.550	4
$01\bar{1}7$	2.654	2.648	8	$20\bar{2}11$	1.552		
$11\bar{2}4$	2.503	2.505	10*	$21\bar{3}8$	1.531	1.533	1
$01\bar{1}8$	2.408	2.410	1	$01\bar{1}14$	1.506	—	—
$02\bar{2}2$	2.373	2.375	1	$03\bar{3}6$	1.483	—	—
$02\bar{2}3$	2.308	2.311	4	$21\bar{3}9$	1.473	—	—
$02\bar{2}4$	2.225	2.230	1	$22\bar{4}0$	1.403		
00010	2.218			$02\bar{2}13$	1.396	1.404	5
$02\bar{2}5$	2.131	2.131	6	$22\bar{4}2$	1.392		
$02\bar{2}6$	2.030	2.030	5	$22\bar{4}4$	1.360	—	—
$02\bar{2}7$	1.928	—	—	$21\bar{3}11$	1.358	—	
$10\bar{1}11$	1.862	—	—	$20\bar{2}14$	1.327	1.327	2
$20\bar{2}8$	1.827	—	—				

* Coincidence with tungsten carbide.

Petrology. The main mineral constituents of the calc-silicate rock are grossular, anorthite, and (clino)zoisite. The presence of spinel and hibonite and the absence of quartz indicate the silica-deficient character of the assemblage. The following reaction equation may be written for the phases present in the assemblage:

$$6 \text{ anorthite} + 2 \text{ grossular} + \text{corundum} + 3\ H_2O \rightleftharpoons 6 \text{ zoisite}.$$

TABLE IV. *Unit-cell constants of hibonite*

Locality	*a* (Å)	*c* (Å)	Ref.
Esiva, Madagascar	5.61	22.15	1
Esiva, Madagascar	5.597	22.20	2
Gornaya Shoriya, USSR	5.59	22.2	3
Furua, Tanzania	5.61	22.18	4
Leoville meteorite	5.57	22.01	5
Synthetic $CaO \cdot 6Al_2O_3$	5.56	21.89	6

1. Curien *et al.* (1956).
2. Keil and Fuchs (1971).
3. Yakovlevskaya (1961).
4. This study.
5. Keil and Fuchs (1971).
6. Kato (1967).

The equilibrium pressure-temperature curve pertinent to this reaction is well documented (Newton, 1965; Boettcher, 1970; Perkins *et al.*, 1979). Newton (1965) used natural zoisite, anorthite, and grossular as starting materials for his hydrothermal experiments with, respectively, 1.50 wt% Fe_2O_3, 0.24 wt% Na_2O, and 1.70 wt% ($FeO + Fe_2O_3$) as major impurities. The electron-microprobe analyses of low-Fe zoisite and anorthite in specimen C-76 approach the compositions of the minerals used in these experiments. The composition of the analysed garnet deviates considerably from the nearly pure grossular in containing about 20 mole% almandine. It may be argued, however, that this rather high almandine content will not significantly change the position of the equilibrium PT-curve as indicated by Huckenholz *et al.* (1975), who state that the stability fields of almandine and grossular correspond closely over a pressure range of 2 to 6 kb with a difference in temperature of less than 30 °C.

A further complication concerns the unknown ratio of P_{H_2O}/P_{total}. Low partial pressures of water are indicated by the abundance of high-density carbonic fluid inclusions in the surrounding rocks. Lowering of P_{H_2O} relative to P_{total} will extend the stability field of the grossular-anorthite assemblage. Holdaway (1966) experimentally determined the PT-curve for the zoisite + quartz breakdown reaction under conditions of $P_{H_2O} = P_{total}$, and calculated the influence of a reduction of P_{H_2O} to 0.5 and 0.25 P_{total}. The influence of P_{H_2O} upon the position of the zoisite breakdown reaction in the silica-deficient system under investigation is less well known, but it seems reasonable to use equal shifts of the PT-curve to those calculated by Holdaway (1966) for the silica-saturated system. This results in a position of the $P_{H_2O} = 0.25$. P_{total} curve near the high-pressure limits of the inferred

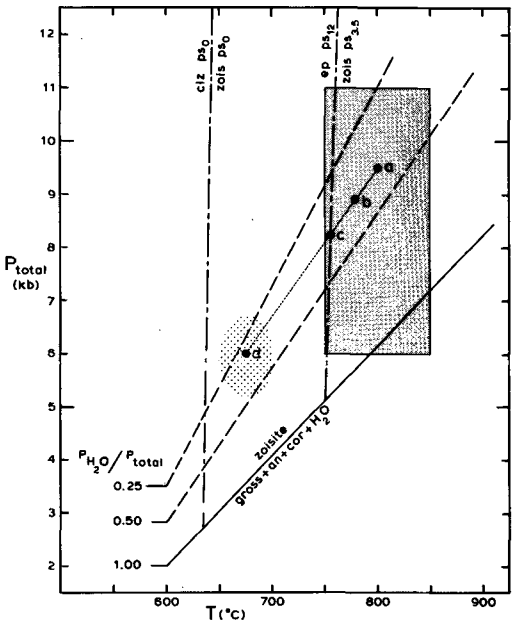

FIG. 6. *PT* diagram with schematic evolutionary path for the calc-silicate assemblage. Shaded field indicates the inferred *PT* field for the regional granulite-facies conditions. Dotted area indicates retrogressive amphibolite-facies conditions. Solid line represents the zoisite-forming reaction curve as given by Newton (1965). Dashed lines are inferred reaction curves for the zoisite-forming reaction under conditions of $P_{H_2O} < P_{total}$, using the data of Holdaway (1966). Dash-dot lines represent the transformation of zoisite to clinozoisite and of zoisite to epidote as given by Holdaway (1972). The points a, b, c, and d mark the various stages of zoisite and clinozoisite growth. For further explanation see text.

field of *PT*-conditions for the main phase of regional metamorphism (fig. 6).

The occurrence of coexisting zoisite and clinozoisite of similar composition and the deviations from the orthorhombic symmetry noted in several zoisite grains indicate that *PT*-conditions prevailed at or near the transformation of orthorhombic to monoclinic symmetry, orthorhombic zoisite being the high-temperature polymorph (Holdaway, 1972). The transformation will lie between the clinozoisite-(Ps-0)/zoisite-(Ps-0) and the epidote-(Ps-12)/zoisite-(Ps-3.5) curves of Holdaway (1972), presumably nearer to the latter curve in view of the composition of the analysed zoisite and clinozoisite (Ps = pistacite content). This would place the orthorhombic-monoclinic transformation roughly between the amphibolite and the granulite metamorphic facies.

Retrograde metamorphism (at lower temperatures and pressures, higher partial water pressures, and an enhanced Fe^{3+}-activity) will decrease the stability field of the grossular-anorthite-corundum assemblage, and will yield intermediate-Fe type clinozoisite as rims and small hypidiomorphic grains around grossular and anorthite.

On the basis of the data presented above a genetic model for the course of events is proposed which reflects a steady decrease in temperature and load pressure and an increase in partial H_2O pressure (fig. 6):

(*a*) formation of a granulite-facies assemblage of grossular-anorthite-hibonite-allanitic clinozoisite-(± granular low-Fe zoisite);

(*b*) growth of low-Fe zoisite poikiloblasts and hypidiomorphic prisms;

(*c*) transformation of zoisite to clinozoisite;

(*d*) retrograde metamorphism under amphibolite-facies conditions with growth of intermediate-Fe clinozoisite and alteration of hibonite.

The Tanzania hibonite appears to be a stable phase in granulite-facies assemblages of suitable silica-deficient and Ca-Al-rich lithologies. Alteration occurs during increase of partial water pressures under retrogressive amphibolite-facies conditions. The Siberia hibonite, in contrast, is a stable phase in amphibolite-facies assemblages, a fact which may be explained by the calcareous composition of the rock.

The differences in the chemical composition between terrestrial and meteoritic hibonites, as shown mainly by the relatively high *RE* and/or Th contents of the former, may be an expression of different temperature and pressure conditions of formation of hibonite in both environments.

Acknowledgements. This investigation was supported by a grant of the Netherlands Foundation for the Advancement of Tropical Research (WOTRO) administered to Maaskant and Coolen. Electron-microprobe facilities were provided by the Free University and the WACOM, a working group for analytical geochemistry subsidized by the Netherlands Organization for the Advancement of Pure Research (ZWO). Field-work in Tanzania was authorized by Mr D. C. Chao, Principal Geologist of the Geology and Mines Division at Dodoma. Dr C. Guillemin, École Nationale Supérieure des Mines, Paris, provided a specimen of the Madagascar hibonite. Thanks are further due to Dr H. van Lamoen for his useful comments and his review of the manuscript and to Dr J. C. Lorin, Université Pierre et Marie Curie, Paris, for detailed information on meteoritic hibonite.

REFERENCES

Ackermand (D.) and Raase (P.), 1973. Coexisting zoisite and clinozoisite in biotite schists from the Hohe Tauern, Austria. *Contrib. Mineral. Petrol.* **42**, 333-41.

Blander (M.) and Fuchs (L. H.), 1975. Calcium-aluminium-rich inclusions in the Allende meteorite.

Evidence for a liquid origin. *Geochim. Cosmochim. Acta*, **39**, 1605–9.

Boettcher (A. L.), 1970. The system CaO–Al_2O_3–SiO_2–H_2O at high pressures and temperatures. *J. Petrol.* **11**, 337–79.

Coolen (J. J. M. M.), 1980. Chemical petrology of the Furua Granulite Complex, southern Tanzania. Ph.D. thesis, Free Univ. Amsterdam. *GUA Papers of Geology*, Ser. 1, 13, 258 pp.

Curien (H.), Guillemin (C.), Orcel (J.), and Sternberg (M.), 1956. La hibonite, nouvelle espèce minérale. *C.R. Acad. Sci. Paris*, **242**, 2845–7.

Hasegawa (S.), 1960. Chemical composition of allanite. *Sci. Report Tohoku Univ. Ser. 3 (Mineral. Petrol. Econ. Geol.)*, **6**, 331.

Hepworth (J. V.), 1972. Charnockitic granulites of some African cratons. *24th Internat. Geol. Congr. Montreal*, Section 1, 126–34.

Holdaway (M. J.), 1966. Hydrothermal stability of clinozoisite plus quartz. *Am. J. Sci.* **264**, 643–67.

—— 1972. Thermal stability of Al-Fe epidote as a function of f_{O_2} and Fe content. *Contrib. Mineral. Petrol.* **37**, 307–40.

Huckenholz (H. G.), Hölzl (E.), and Lindhuber (W.), 1975. Grossularite, its solidus and liquidus relations in the CaO–Al_2O_3–SiO_2–H_2O system up to 10 kbar. *Neues Jahrb. Mineral. Abh.* **124**, 1–46.

Kato (K.), 1967. Strukturverfeinerung von $CaO \cdot 6Al_2O_3$. *Naturwiss.* **54**, 536.

Keil (K.) and Fuchs (L. H.), 1971. Hibonite [$Ca_2(Al,Ti)_{24}O_{38}$] from the Leoville and Allende chondritic meteorites. *Earth Planet. Sci. Lett.* **12**, 184–90.

Kieft (C.) and Maaskant (P.), 1969. Quantitative microprobe-analyses of silicates: a comparison of different correction methods. *Abstr. Confer. Roy. Microsc. Soc. Roy. Mineral. Soc. Manchester.*

Kröner (A.), 1977. The Precambrian geotectonic evolution of Africa: plate accretion versus plate destruction. *Precambrian Res.* **4**, 163–213.

—— 1979. Pan-African mobile belts as evidence for a transitional tectonic regime from intraplate orogeny to plate margin orogeny. *In* Al Shanti (A. M. S.) (ed.), *Evolution and mineralization of the Arabian-Nubian Shield.* Oxford, Pergamon Press, pp. 21–37.

Kuzmin (A. M.), 1960. Högbomite from Gornaya Shoriya. *Geol. Geof.* **4**, 63–75.

Letuvninkas (A. I.), 1971. Metasomatism in Proterozoic carbonate rocks from Gornaya Shoriya. *Geol. Geof.* **1**, 58–64.

Macdougall (J. D.), 1979. Refractory-element-rich inclusions in CM meteorites. *Earth Planet. Sci. Lett.* **42**, 1–6.

Moore (A. C.), 1971. Corundum-ilmenite and corundum-spinel associations in granulite facies rocks from central Australia. *J. Geol. Soc. Australia*, **17**, 227–9.

Myer (G. H.), 1966. New data on zoisite and epidote. *Am. J. Sci.* **264**, 364–85.

Newton (R. C.), 1965. The thermal stability of zoisite. *J. Geol.* **73**, 431–41.

Perkins (D., III), Essene (E. J.), Westrum (E. F., *Jr.*), and Wall (V. J.), 1977. Application of new thermodynamic data to grossular phase relations. *Contrib. Mineral. Petrol.* **64**, 137–47.

Priem (H. N. A.), Boelrijk (N. A. I. M.), Hebeda (E. H.), Verdurmen (E. A. Th.), Verschure (R. H.), Oen (I. S.), and Westra (L.), 1979. Isotopic age determinations on granitic and gneissic rocks from the Ubendian-Usagaran System in southern Tanzania. *Precambrian Res.* **9**, 227–39.

Quennel (A. M.), McKinlay (A. C. M.), and Aitken (W. G.), 1956. Summary of the geology of Tanganyika. Part 1: Introduction and stratigraphy. *Tanganyika Geol. Surv. Mem.* **1**, 264 pp.

Shimizu (N.), Semet (M. P.), and Allègre (C. J.), 1978. Geochemical applications of quantitative ion-microprobe analysis. *Geochim. Cosmochim. Acta*, **42**, 1321–34.

Smith (J. V.), 1979. Mineralogy of the planets: a voyage in space and time. *Mineral. Mag.* **43**, 1–89.

Spooner (C. M.), Hepworth (J. V.), and Fairbairn (H. W.), 1970. Whole-rock Rb–Sr isotopic investigation of some East African granulites. *Geol. Mag.* **107**, 511–21.

Springer (G.), 1967. Die Berechnung von Korrekturen für die quantitative Elektronenstrahl-Mikroanalyse. *Fortschr. Mineral.* **45**, 103–24.

Tröger (W. E.), 1971. *Optische Bestimmung der gesteinsbildenden Minerale.* Stuttgart, E. Schweizerbart'sche Verlagsbuchhandlung, 188 pp.

Wendt (I.), Besang (C.), Harre (W.), Kreuzer (H.), Lenz (H.), and Müller (P.), 1972. Age determinations of granitic intrusions and metamorphic events in the Early Precambrian of Tanzania. *24th Internat. Geol. Congr. Montreal*, Section 1, 295–314.

Yakovlevskaya (T. A.), 1961. Hibonite from Gornaya Shoriya. *Zap. Vses. Min. Obshch.* **90**, 458–61.

[*Manuscript received 13 March 1980*]